Self-Assembled Ruthenium(II)Porphyrin-Aluminium(III)Porphyrin-Fullerene Triad for Long-Lived Photoinduced Charge Separation

Agnese Amati,[†] Paolo Cavigli,[†] Axel Kahnt,[∥] Maria Teresa Indelli,[*,‡,§] and Elisabetta Iengo[*,†]

[†]Department of Chemical and Pharmaceutical Sciences, University of Trieste, Via L. Giorgieri 1, 34127 Trieste, Italy
[‡]Department of Chemical and Pharmaceutical Sciences, University of Ferrara, Via Fossato di Mortara 17, 44121 Ferrara, Italy
[§]Centro Interuniversitario per la Conversione Chimica dell'Energia Solare, sezione di Ferrara, via L. Borsari 46, 44121 Ferrara, Italy
[∥]Lehrstuhl für Physikalische Chemie I, Friedrich-Alexander-Universität Erlangen-Nürnberg, Egerlandstraße 3, 91058 Erlangen, Germany

Supporting Information

ABSTRACT: A very efficient metal-mediated strategy led, in a single step, to a quantitative construction of a new three-component multichromophoric system containing one fullerene monoadduct, one aluminium(III) monopyridylporphyrin, and one ruthenium(II) tetraphenylporphyrin. The Al(III) monopyridylporphyrin component plays the pivotal role in directing the correct self-assembly process and behaves as the antenna unit for the photoinduced processes of interest. A detailed study of the photophysical behavior of the triad was carried out in different solvents (CH_2Cl_2, THF, and toluene) by stationary and time-resolved emission and absorption spectroscopy in the pico- and nanosecond time domains. Following excitation of the Al–porphyrin, the strong fluorescence typical of this unit was strongly quenched. The time-resolved absorption experiments provided evidence for the occurrence of stepwise photoinduced electron and hole transfer processes, leading to a charge-separated state with reduced fullerene acceptor and oxidized ruthenium porphyrin donor. The time constant values measured in CH_2Cl_2 for the formation of charge-separated state Ru-Al$^+$-C$_{60}^-$ (10 ps), the charge shift process (Ru-Al$^+$-C$_{60}^-$ → Ru$^+$-Al-C$_{60}^-$), where a hole is transferred from Al-based to Ru-based unit (75 ps), and the charge recombination process to ground state (>5 ns), can be rationalized within the Marcus theory. Although the charge-separating performance of this triad is not outstanding, this study demonstrates that, using the self-assembling strategy, improvements can be obtained by appropriate chemical modifications of the individual molecular components.

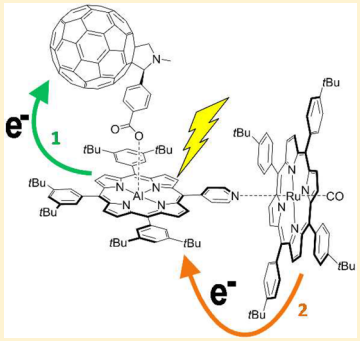

INTRODUCTION

Artificial photosynthesis, that is, the conversion of solar energy into fuels, is an attractive potential solution to the global energy problem.[1−11] Mimicking natural photosynthesis, artificial systems featuring light-driven functions, like the antenna effect[12−21] and charge-separation,[22−27] have been thoroughly studied in recent years. As these functions generally rely on the occurrence of very specific sequences of intercomponent energy or electron transfer elementary steps, a very precise spatial organization of molecular components (chromophores, electron donors, and acceptors) must be synthetically achieved. In this context, we have previously synthesized a series of multicomponent arrays with the desired photoinduced properties by self-assembly of appropriate subunits.[21−25] In particular, some years ago we described the quantitative self-assembly of a photoactive nonsymmetric triad obtained from the axial coordination of a naphthalenediimide (electron acceptor unit), to an aluminium(III) porphyrin (central photoexcitable sensitizer) which, in turn, is axially bound to a ruthenium(II) porphyrin (electron donor unit) (**NDI–AlMPyP–RuP**, Chart 1).[23] The selective affinity of the two different metal centers, aluminium (hard center) and ruthenium (soft center) toward

Chart 1. Triad System NDI–AlMPyP–RuP

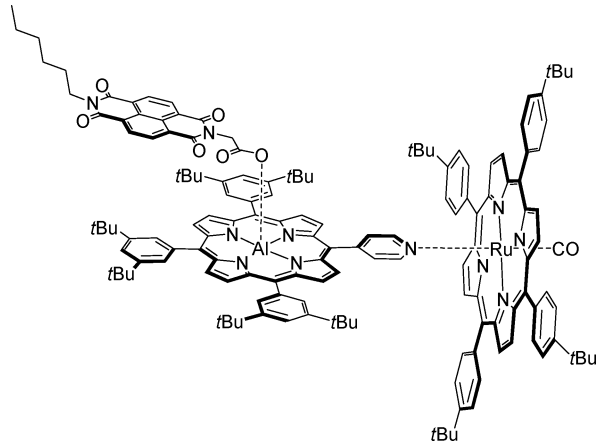

oxygen or nitrogen ligands, respectively, is crucial for the efficient self-sorting of the desired three-component product.

Ultrafast spectroscopy experiments upon excitation of the aluminium porphyrin provide clear evidence for the occurrence of stepwise electron (3 ps) and hole transfer (35 ps), leading to a charge-separated state with reduced acceptor and oxidized donor (NDI^{-}-AlMPyP-RuP^{+}), with a lifetime in the few nanoseconds range. More recently, aluminium(III) porphyrins have been successfully used by van der Est and co-workers as chromophoric units for constructing several triads performing long-lived light-induced charge separation by sequential electron transfer.[27−30] In particular, they reported an important and thorough photophysical study using both time-resolved absorption and EPR technique on a series of linear systems where tetrathiafulvalene as a donor and a fullerene unit as an acceptor are bound to the aluminium center on opposite faces of the porphyrin with bridges of different length.[30] These systems, although structurally different from the triad of Chart 1, were designed for the same purpose, that is, to take advantage of the distinctive properties of aluminium(III) porphyrin chromophoric component to obtain photoinduced charge-separating triad systems. In the present work, to improve the performance of this type of system, we have pursued the preparation of a new triad where we have varied the nature of one of the building blocks, replacing the naphthalenediimide with a C_{60} component (Chart 2).

Chart 2. Triad System C_{60}-AlMPyP-RuP

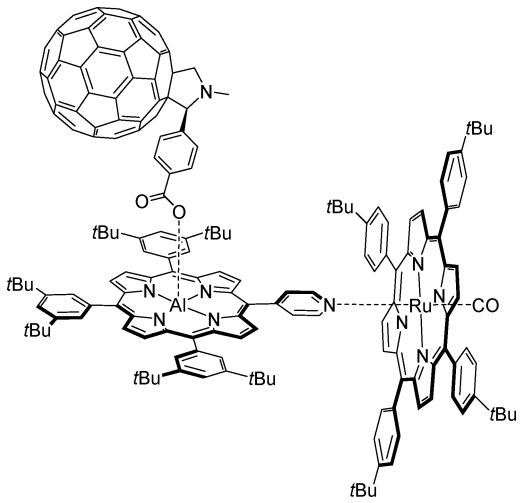

This component has been widely used by several groups as an electron acceptor in the design of artificial photosynthetic systems[31−41] given its peculiar and useful properties: (i) low and reversible first reduction potential and (ii) small reorganization energy, which tends to increase the rate of charge separation and decrease that of charge recombination.[42−45]

In this work, we report the synthesis and characterization in different solvents of this new triad. The photophysics is thoroughly investigated by time-resolved techniques in the picosecond time domain, with particular attention to the photoinduced charge separation, hole transfer, and recombination processes.

EXPERIMENTAL SECTION

Materials. All reagents were purchased from Sigma-Aldrich and used without further purification. Spectroscopic grade and electrochemical grade solvents were used for the photophysical and electrochemical measurements. Deuterated dichloromethane was purchased from CIL. 5-(4′-Pyridyl)-10,15,20-(phenyl)-porphyrin (**MPyP**) and *meso*-tetraphenylporphyrin (**TPP**) were synthesized and purified according to literature methods.[46] 5-(4′-Pyridyl)-10,15,20-(3,5-di-*tert*-butylphenyl)-porphyrinato-(hydroxo)aluminium(III) (**AlMPyP**),[23] *meso*-(4-*tert*-butyl)-tetraphenylporphyrinato-(carbonyl)ruthenium(II) (**RuP**),[47] and 1-methyl-2-(4-carboxybenzyl)-3,4-fulleropyrrolidine ($\mathbf{C_{60}}$)[27] were synthesized and purified as described in the literature. The model compounds, *meso*-(4-*tert*-butyl)-tetraphenylporphyrinato-(pyridyl-carbonyl)ruthenium(II) **RuP(py)**[48] and *meso*-(3,5-di-*tert*-butyl)-tetraphenylporphyrinato-(benzoate)aluminium(III) **AlP(ba)**,[49] were prepared as previously reported.

Instrumental Methods. Mono- and bidimensional NMR experiments (^{1}H, H−H COSY, H−C COSY) were recorded on a Varian 500 (500 MHz) spectrometer. All spectra were run at room temperature; ^{1}H chemical shifts were referenced to the peak of residual nondeuterated solvent [δ (ppm) = 5.31 (CH_2Cl_2)]. Infrared spectra were recorded on a PerkinElmer FT-IR 2000 spectrometer in the transmission mode, and the samples were prepared as KBr pellets.

UV−vis absorption spectra were recorded on a Jasco V-570 UV/vis/NIR spectrophotometer. Emission spectra were acquired on a Horiba-Jobin Yvon Fluoromax-2 spectrofluorimeter, equipped with a Hamamatsu R3896 tube. Fluorescence lifetimes were measured using a time-correlated single photon counting (TSPC) apparatus (PicoQuant Picoharp 300) equipped with subnanosecond LED sources (280, 380, 460, and 600 nm; 500−700 ps pulse width) powered by a PicoQuant PDL 800-B variable (2.5−40 MHz) pulsed power supply. The decays were analyzed by means of PicoQuant FluoFit Global fluorescence decay analysis software.

Transient absorption experiments based on femtosecond laser photolysis were performed using two different setups. (1) In Erlangen, the measurements were carried out using an amplified Ti/sapphire laser system CPA-2111 fs laser (Clark MXR, output: 775 nm, 1 kHz, and 150 fs pulse width) with a transient absorption pump/probe detection system equipped with a visible and NIR detector (TAPPS Helios, Ultrafast Systems). The excitation wavelength (550 nm) was generated with an NOPA Plus (Clark MXR); pulse widths < 150 fs with an energy of 200 nJ were selected. (2) In Ferrara, the measurements were performed using a pump−probe setup based on a Hurricane Spectra-Physics Hurricane Ti:sapphire laser source (fwhm = ca. 130 fs) and Ultrafast Systems Helios spectrometer equipped with a TAPPS-Helios with a detection range between 450 and 800 nm (Ultrafast Systems) transient absorption spectrometer. The excitation pulses (590 nm) were generated with an OPA (Spectra Physics 800 OPA). Probe pulses were obtained by continuum generation on a sapphire plate (useful spectral range: 450−800 nm). Effective time resolution ca. 200 fs, and a temporal window of the optical delay stage of 0−2000 ps. The time-resolved spectral data were deconvoluted to correct for spectral chirp and thus analyzed with Ultrafast Systems Surface Explorer Pro.[50]

Cyclic voltammetric measurements were carried out with a PC-interfaced EcoChemie Autolab/Pgstat30 Potentiostat.

Scheme 1. Self-Assembly of the Three-Component System C_{60}-AlMPyP-RuP from the Starting Building Units C_{60}, AlMPyP, and RuP

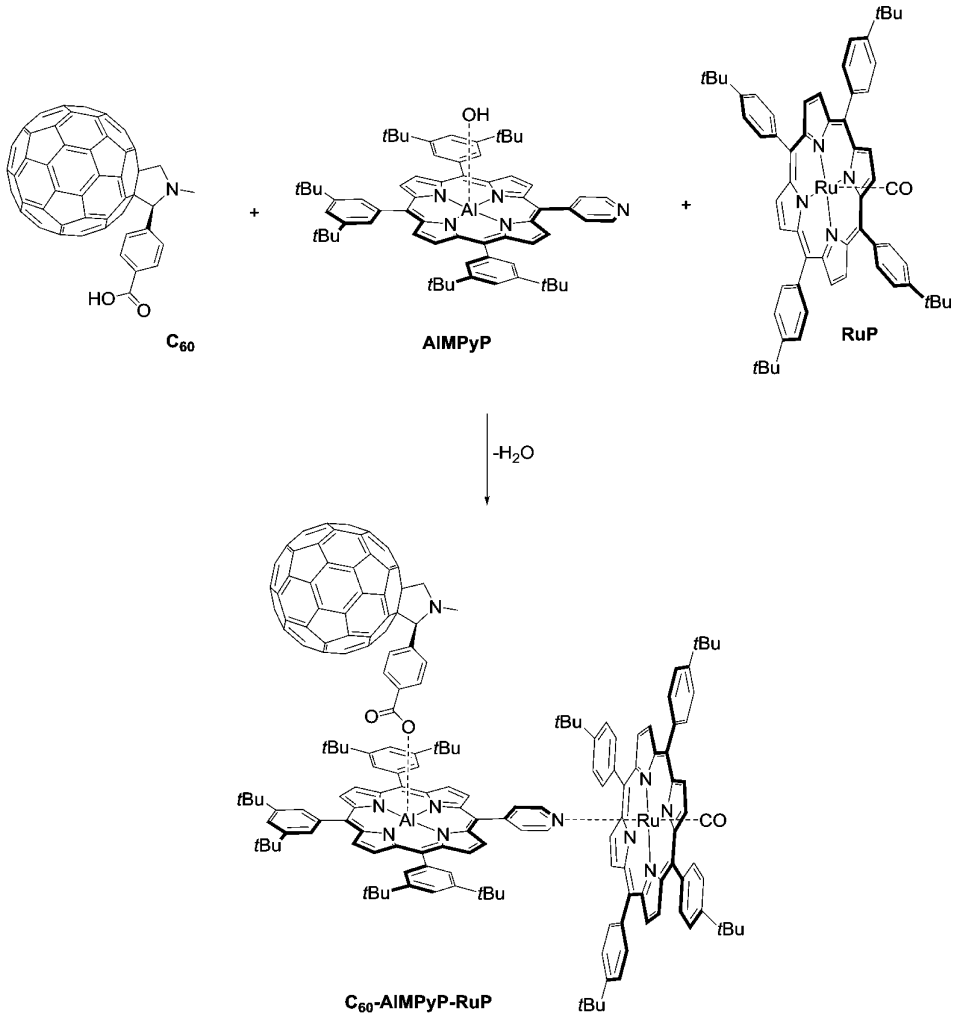

Argon-purged solutions in CH_2Cl_2 (Romil, Hi-dry) containing 0.1 M (TBA) (PF_6) (TBA = tetrabutylammonium, Fluka, electrochemical grade; dried in oven) were used. A conventional three-electrode cell assembly was used.

Synthesis of C_{60}-AlMPyP-RuP. **AlMPyP** (14.9 mg, 0.015), **RuP** (14.5 mg, 0.015 mmol), and **C_{60}** (13.5 mg, 0.015 mmol) were dissolved in chloroform (30 mL). The solution was stirred at room temperature for a few minutes, and the solution turned from red-violet to violet almost instantly. The concentration of the solution in vacuo to approximately half of its original volume and the subsequent addition of *n*-hexane induced the precipitation of the product as a red-violet powder, which was collected by filtration, washed with *n*-hexane, and vacuum-dried. Yield 40.5 mg (95%). ^{1}H NMR (δ, 500 MHz, CD_2Cl_2): 9.05−8.91 (m, 4H, β_{4Al}+ β_{3Al}), 8.78 (s, 8H, β_{Ru}), 8.74−8.69 (m, 2H, β_{2Al}), 8.26 (d, J = 7.9 Hz, 4H, o_{Ru}), 8.12 (d, J = 7.9 Hz, 4H, o'_{Ru}), 8.05−7.87 (br, m, 6H, o_{Al}+o'_{Al}), 7.82 (d, J = 8.0 Hz, 4H, m_{Ru}), 7.79 (s, 3H, p_{Al}+p'_{Al}), 7.72 (d, J = 7.9 Hz, 4H, m_{Ru}), 7.52 (d, J = 4.9 Hz, 2H, β_{1Al}), 6.69 (br, s, 2H, b), 6.00 (d, J = 5.5 Hz, 2H, py_b), 4.81(d, J = 7.9 Hz, 2H, a), 4.61 (d, J = 9.4 Hz, 1H, H_B), 4.29 (s, 1H, H_A), 3.87 (d, J = 9.4 Hz, 1H, H_C), 2.20 (s, 3H, CH_3), 1.89 (d, J = 5.3 Hz, 2H, py_a), 1.60 (s, 36H, tBu$_{Ru}$), 1.44 (s, 54H, tBu$_{Al}$). ^{13}C NMR (δ, HSQC, CD_2Cl_2): 142.42 (C_{aAl}), 133.96 (C_{oHRu}), 132.46 ($C_{\beta 4Al}$), 132.25 ($C_{\beta 3Al,\ \beta 2Al}$), 131.87 ($C_{\beta Ru}$), 129.64 ($C_{\beta 1Al}$), 129.10 ($C_{oHAl}$), 126.49 ($C_{bAl}$), 123.55 ($C_{mHRu}$), 123.27 ($C_{mHRu}$), 121.50 ($C_{pHAl}$), 39.03 ($C_{CH3C60}$), 31.20 ($C_{tBuRu,tBuAl}$). Selected IR bands (cm^{-1}, KBr pellets, Figure S1): 1952 (s, $\nu_{C=O}$), 1592 (s, $\nu_{C=Oacid}$). UV−vis (λ_{max}, nm, CH_2Cl_2): 416, 542, 587sh, 638.

RESULTS AND DISCUSSION

Synthesis and Characterization. The quantitative and selective one-pot self-assembly of the three-component photoactive system **C_{60}-AlMPyP-RuP** was efficiently achieved at room temperature by simply mixing the individual compounds (in a stoichiometric ratio) in CH_2Cl_2 solution as reported in Scheme 1.

In particular, the coordination of the carboxylic group to the Al(OH)-porphyrins occurs with the loss of one molecule of H_2O, which leads to the attachment of a benzoate group. **C_{60}-AlMPyP-RuP** was fully characterized in solution by means of one-dimensional (1D) and two-dimensional (2D) NMR experiments (Figure 1 and Figures S2 and S3). In Figure 1, the proton NMR spectrum of the adduct is reported. All the assignments were made by means of 2D experiments, and the corresponding resonances show the correct relative integrations. As demonstrated in previous works,[23,26] the proton resonances of the benzoate moiety of the fullerene ligand ($H_{3,5}$ and $H_{2,6}$) and the resonances of the beta protons (β_{1-4}) and of

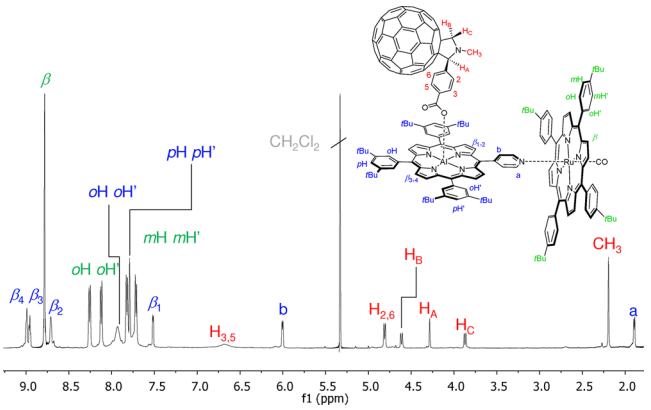

Figure 1. ^{1}H NMR (500 MHz, CD_2Cl_2) spectrum of **C_{60}-AlMPyP-RuP**.

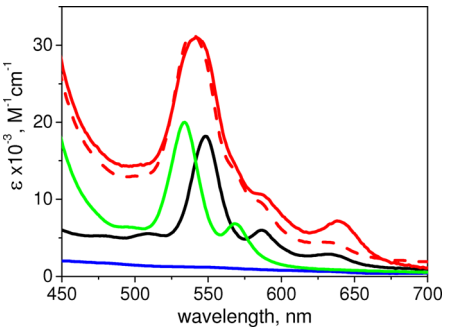

Figure 3. Absorption spectra in the visible region of **C_{60}-AlMPyP-RuP** (continuous red line) and of its molecular components (**AlP(ba)**, black line, **RuP(py)**, green line, and **C_{60}** blue line) in CH_2Cl_2. The arithmetic sum of the spectra of the three components is also reported (dotted red line).

the protons of the pyridyl group (a and b) of the aluminium porphyrin unit show an upfield shift due to the shielding cone of the porphyrin macrocycles.

Stability in Solution, Spectroscopic and Electrochemical Properties. The spectroscopic and the electrochemical behavior of the self-assembled system was thoroughly investigated in comparison with model compounds representative of the individual components namely **C_{60}**, **AlP(ba)** and **RuP(py)** (see Figure 2).

As already observed for related side-to-face and axially coordinated assemblies,[23−25] the triad **C_{60}-AlMPyP-RuP** system of this work is truly supramolecular in nature as demonstrated by the appreciable additivity of the absorption spectra of the component subunits and of the redox properties (vide infra). The selective affinity of the two different metalloporphyrin toward nitrogen (Ru(II) porphyrin) or oxygen (Al(III) porphyrin) ligands, together with the inert nature of the established coordination bonds, guarantee a high stability of the assembly. All the photophysical experiments refer to freshly prepared solutions at concentrations higher than 5×10^{-5} M. In these conditions, the array studied was found to be intact as checked by concentration-dependent spectrofluorimetric measurements.[23]

The absorption spectrum of the triad **C_{60}-AlMPyP-RuP** (Figures S4 and S5) measured in the UV and visible regions is a good superposition of those of the molecular components, clearly indicating the supramolecular nature of the system studied. The spectrum of **C_{60}-AlMPyP-RuP** in the visible region is shown in Figure 3.

The optical absorptions of **AlMPyP** and **RuP** chromophoric units are overlapping with Soret bands around 420 nm and Q-bands between 500 and 700 nm.[51] In this region, the contribution of the fullerene unit is totally negligible.

Taking the former into account, selective excitation of the single chromophores is not feasible. However, the supramolecular character of the system permits a reasonable estimation of the amount of light absorbed by the two types of chromophores at different wavelengths. In practice, 550 and 590 nm were found to be convenient wavelengths for the efficient (70% and 90%, respectively) excitation of the **AlMPyP** component. The spectral features of Figure 3 remain almost unchanged by changing the solvent from dichloromethane to toluene (Figures S4 and S5), the only difference being a small blue shift (2−3 nm) for the Q-bands.

The electrochemical properties of the **C_{60}-AlMPyP-RuP** triad were examined by cyclic voltammetry (CV, electrochemical window from +1.5 to −1.5 V) in a CH_2Cl_2 solution (Figure S6). For comparison, the model compounds were studied in the same experimental conditions. The results are summarized in Table 1. As expected by a comparison with similar systems,[23−25] this voltammetric behavior is a good superposition of those of the molecular components, confirming the supramolecular nature of the system investigated. For example, in the triad, the two reductions of the fullerene units, the reduction of the aluminium porphyrin, the oxidation of the ruthenium porphyrin, and the oxidation of the aluminium porphyrin can easily be assigned as their potentials

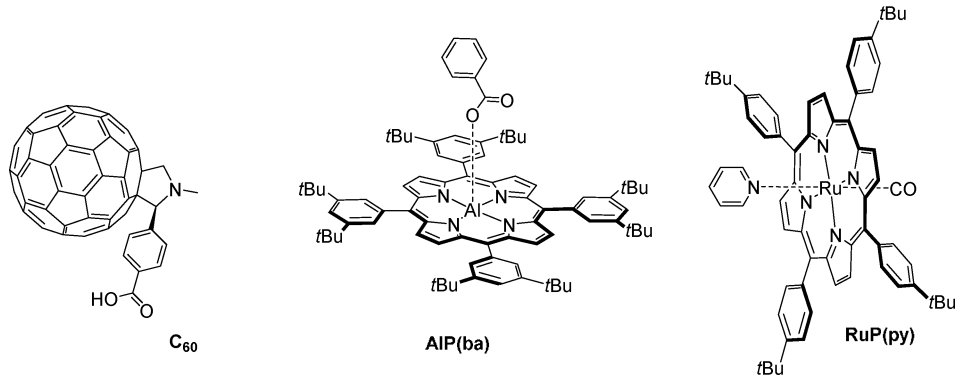

Figure 2. Schematic representation of the model compounds: **C_{60}**, **AlP(ba)**, and **RuP(py)**.

Table 1. Electrochemical Data for C_{60}-AlMPyP-RuP and the Reference Compounds[a]

	reduction			oxidation	
AlP(ba)[b]	− 1.21			+ 0.88	
RuP(py)[b]				+ 0.78	
C_{60}	−1.04	− 0.65			
C_{60}-AlMPyP-RuP	−1.21	− 1.07	− 0.67	+ 0.77	+ 0.96

[a]All measurements were made in argon deaerated CH_2Cl_2 solutions at 298 K, 0.1 M TBA(PF_6) as the supporting electrolyte, scan rate 200 mV/s, SCE as the reference electrode, ferrocene (0,46 V vs SCE) as the internal standard, and glassy carbon as the working electrode. Half wave potential in cyclic voltammetry (ΔE_p = 60−80 mV). [b]Ref 23.

are practically identical, within experimental error, to those of the constituent units.

Photophysical Characterization of the C_{60}-AlMPyP-RuP Triad. The photophysical behavior of the new triad was thoroughly investigated in dichloromethane, THF, and toluene, upon visible excitation, by steady-state and time-resolved absorption and emission spectroscopy, also in comparison with that of model compounds.

Emission Measurements. At room temperature, a solution of the triad showed the typical Al-porphyrin fluorescence with prominent vibronic bands at 608 and 650 nm (Figure 4); even when taking a close look into the 700−750 region, no C_{60}-centered fluorescence was observed, either in CH_2Cl_2 or in less polar solvents (e.g., toluene).[52]

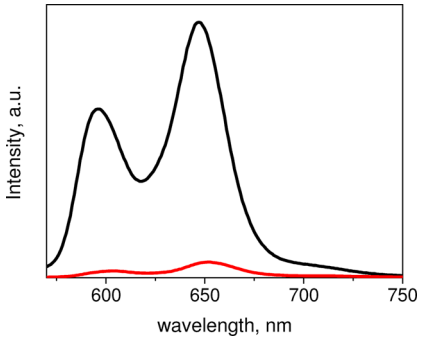

Figure 4. Emission spectra of the triad (red line) and **AlP(ba)** model compound (black line) under the same experimental conditions (λ_{exc} = 550 nm) at room temperature in a CH_2Cl_2 solution.

Comparative experiments, carried out on optically matched solutions of the triad and the **AlP(ba)** model at λ_{exc} = 550 nm, indicate that, in the triad, the intense fluorescence characteristic of the Al-porphyrin unit, although maintaining the same emission pattern, is strongly quenched ($\Phi_0/\Phi \geq 90$, where Φ_0 and Φ are the fluorescence quantum yields of the **AlP(ba)** model and of the triad, respectively) (Figure 4). Single photon counting experiments demonstrate that the lifetime of the residual fluorescence lies below the instrumental resolution of the TC-SPC technique (i.e., < 250 ps) (Figure S7) clearly indicating that, in the triad system, the fluorescence lifetime is dramatically quenched compared with the **AlP(ba)** model.[53]

Ultrafast Transient Absorption Spectroscopy. To access shorter time scales and obtain insights into the quenching mechanism, ultrafast transient absorption experiments were performed in different solvents (dichloromethane, toluene, and tetrahydrofuran) using different experimental setups and excitation wavelengths.

In order to interpret the results, it is useful to construct a simplified energy level diagram for the triad (Figure 5), where,

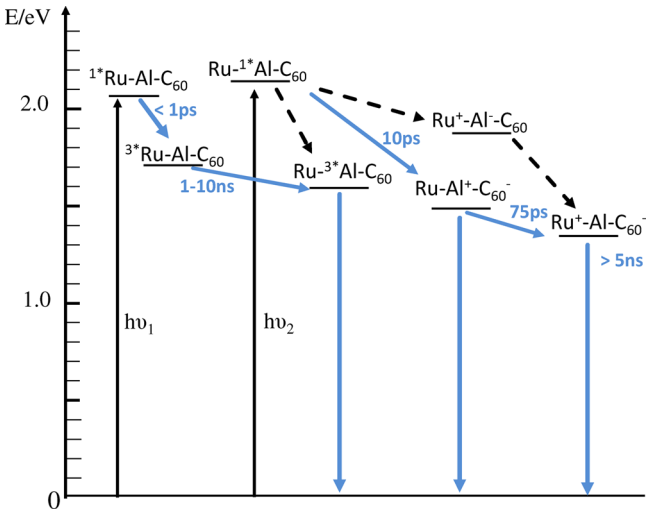

Figure 5. Energy diagram and photophysical mechanisms for the **C_{60}-AlMPyP-RuP** triad in CH_2Cl_2. Shorthand notation: AlMPyP = Al and RuP = Ru.

besides the localized excited states of the Ru-based and Al-based chromophores,[54−56] three intercomponent charge separated states must be considered: (i) a state in which the ruthenium-based unit is oxidized and the aluminium-based unit is reduced (Ru^+-Al^--C_{60}), (ii) a state in which the aluminium-based unit is oxidized and the C_{60} unit is reduced (Ru-Al^+-C_{60}^-), and (iii) a state in which the ruthenium-based unit is oxidized and a C_{60} unit is reduced (Ru^+-Al-C_{60}^-). The energy of these states in CH_2Cl_2 solution can be calculated from the measured redox potentials (Table 1) with appropriate correction for the electrostatic work term estimated according to standard procedures.[57,58] Within the limits of this type of calculation, Ru^+-Al^--C_{60} is estimated to lie at 1.83 eV, Ru-Al^+-C_{60}^- at 1.53 eV, and Ru^+-Al-C_{60}^- at 1.34 eV.

From inspection of this energy level diagram (Figure 5), it appears immediately clear that, upon excitation of the **AlMPyP** chromophore, various quenching pathways are thermodynamically feasible in this system. Ultrafast spectroscopy experiments are crucial to establish the processes responsible for the photophysical deactivation of the triad. Transient absorption spectra in CH_2Cl_2 obtained at different time delays upon excitation at 550 nm are shown in Figure 6.

The initial spectrum, taken immediately after the laser pulse (t = 1 ps) (Figure 6a), is the typical spectrum of the Al−porphyrin unit singlet excited state.[23,30] It is characterized by (i) an intense absorption band peaking at 455 nm, (ii) a broad positive absorption at longer wavelengths (600−720 nm), with superimposed apparent bleaches at 600 and 650 nm caused by stimulated emission, and (iii) a broad positive absorption in the 1200−1350 nm region peaking at 1240 nm.[59] The transient spectral changes show a triphasic behavior, with different spectral changes taking place in the 1−25 ps (Figure 6a), in the 25−200 ps (Figure 6b), and in 200−5000 ps time ranges (Figure 6c). In the early time scale (1−25 ps, Figure 6a), absorption features due to the disappearance of the singlet excited state of **AlMPyP** unit (the disappearance of the stimulated emission and a reduction in the absorption bands at 455 nm and at 1240 nm), and to the formation of the radical

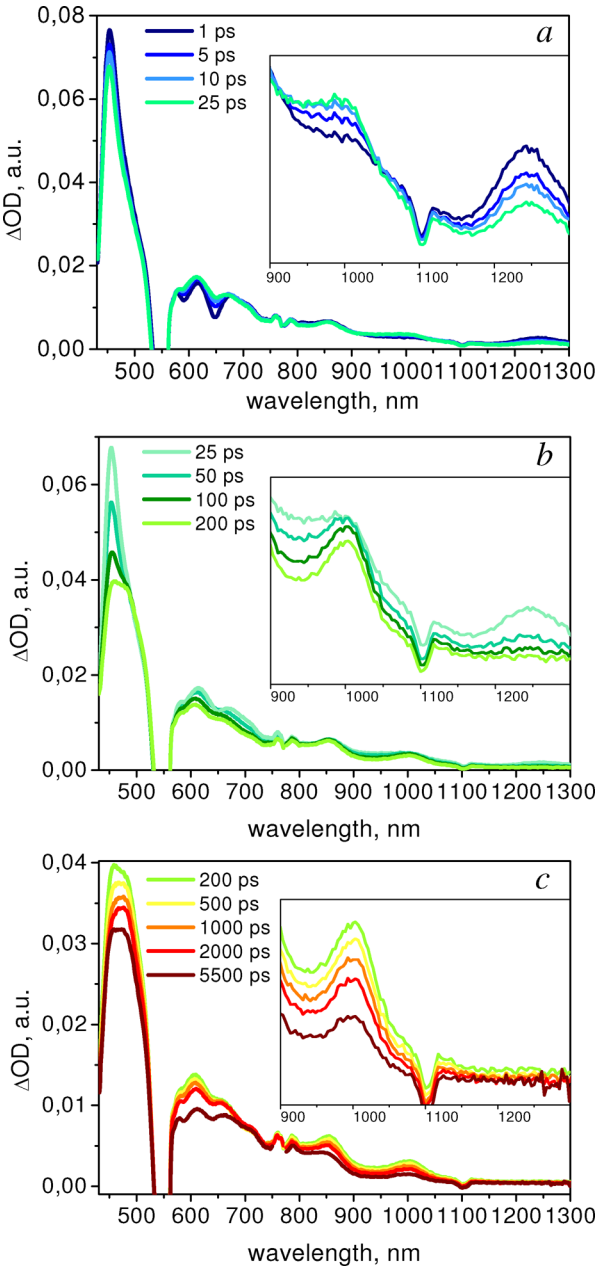

Figure 6. Transient absorption spectra obtained by the ultrafast spectroscopy (excitation at 550 nm) in CH_2Cl_2 in the (a) 1−25 ps time range, (b) 25−200 ps range, (c) and 200−5500 ps range. Inset: the transient spectra in the 900−1300 nm spectral window are multiplied by a factor of 10.

cation of **AlMPyP** unit (an increase in a broad absorption band in the 600−650 nm range) together with the formation of the radical anion of $\mathbf{C_{60}}$ component (growth of a characteristic absorption centered around 1000 nm) are clearly discernible. These spectral changes are relatively small, but the signatures of the radical anion of the fullerene unit provide direct evidence for the formation of a charge-separated state in which the **AlMPyP** unit is oxidized and the fullerene is reduced (Ru-Al$^+$-C_{60}^-). Importantly, the Ru-Al$^+$-C_{60}^- features grow in a time scale that matches the decay of the **AlMPyP** singlet excited state, confirming that, in less than 25 ps after excitation, a photoinduced electron-transfer process from the **AlMPyP** excited state to the $\mathbf{C_{60}}$ unit occurs (Figure 6a). Kinetic analysis of the spectral changes at 1240 nm (disappearance of the **AlMPyP** singlet excited state) and at 1003 nm (formation of the radical anion of $\mathbf{C_{60}}$) (Figure 7a) yields a very similar time constant value of ca. 10 ± 5 ps. This value is consistent with that obtained from kinetic analysis at 650 nm (Figure 7b) where the formation of the radical cation of **AlMPyP** is observed.

In the subsequent time range (25−200 ps, Figure 6b), the most evident feature is a strong decrease and a shift to the red of the sharp band at 450 nm. These transient changes are consistent with the disappearance of the **AlMPyP** radical cation together with the formation of the **RuP** radical cation. This species exhibits a broad absorption with a maximum at around 480 nm (see the spectrum of the radical cation of **RuP** obtained in spectroelectrochemical experiments, reported in ref 23). Kinetic analysis of spectral changes at 650 nm (Figure 7b) and at 450 nm (Figure S8) gives a time constant of 75 ± 10 ps for the disappearance of the **AlMPyP** radical cation.

It is important to note that the absorption of the radical anion of $\mathbf{C_{60}}$, easily recognized around 1000 nm, is constant in this time range (25−200 ps, see Figure 6b). In this regard, the transient spectrum recorded with a 100 ps delay is particularly informative because the absorption band, peaking at 1240 nm due to the singlet state of **AlMPyP** unit, has completely disappeared, while the intensity of the signal of C_{60}^- has not changed. Overall, these observations can easily be assigned to the hole charge shift from the **AlMPyP** unit to the **RuP** unit (i.e., from Ru-Al$^+$-C_{60}^- to Ru$^+$-Al-C_{60}^-). This process is sufficiently fast (ca. 75 ps) to compete favorably with primary charge recombination (see energy level diagram, Figure 5).

In the longer time scale (200−5500 ns, Figure 6c), a pronounced decrease in the C_{60}^- signal at 1000 nm clearly indicates that the spectroscopic signatures of the charge-separated state, Ru$^+$-Al-C_{60}^-, start to disappear with a uniform decay of the whole spectrum toward the initial baseline. These transient changes are consistent with the charge recombination of the charge-separated state (Ru$^+$-Al-C_{60}^-) to the ground state (Ru-Al-C_{60}). This process is not complete in the time window of the ultrafast experiments (1−5000 ps), clearly indicating that the long-range charge separated state has a lifetime longer than 5 ns.[60]

In conclusion, as reported in Figure 5 (blue arrows), the interpretation of the ultrafast absorption experiments in CH_2Cl_2 strongly suggests that, following excitation of Al-porphyrin chromophore, the charge separated state Ru-Al$^+$-C_{60}^- is formed in ca. 10 ps (eq 1), a charge shift process Ru-Al$^+$-C_{60}^- → Ru$^+$-Al-C_{60}^-, where a hole is transferred from Al-based to Ru-based unit occurs in ca. 75 ps (eq 2) and the charge recombination process to ground state (eq 3) occurs in a by far longer time scale (>5 ns).

$$\text{Ru-}^{1*}\text{-Al-C}_{60} \rightarrow \text{Ru-Al}^+\text{-C}_{60}^- \quad \Delta G = -0.60 \text{ eV} \qquad (1)$$

$$\text{Ru-Al}^+\text{-C}_{60}^- \rightarrow \text{Ru}^+\text{-Al-C}_{60}^- \quad \Delta G = -0.19 \text{ eV} \qquad (2)$$

$$\text{Ru}^+\text{-Al-C}_{60}^- \rightarrow \text{Ru-Al-C}_{60} \quad \Delta G = -1.34 \text{ eV} \qquad (3)$$

The time constant values experimentally measured can be rationalized within the Marcus theory[61] (assuming approximately similar reorganizational energies): the photoinduced charge-separation and hole-shift processes (eq 1 and eq 2) are relatively fast because the driving forces of the processes place both in the normal Marcus region; moreover, the hole-shift process (eq 2) is slower since it is more activated. On the other

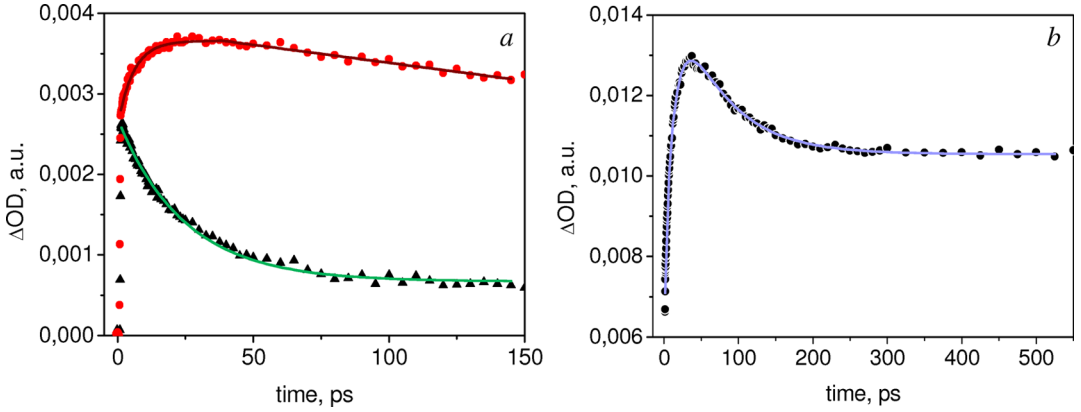

Figure 7. Kinetic analysis of spectral changes in CH_2Cl_2 measured at (a) 1240 nm (▲) and 1003 nm (red ●) and (b) 650 nm.

hand, the charge recombination step (eq 3) is much slower with respect to processes 1 and 2 because, being extremely exergonic, it belongs to the Marcus inverted region.

In order to confirm the right sequence of the electron transfer processes responsible for the quenching of the **AlMPyP** singlet excited state in CH_2Cl_2, ultrafast absorption measurements with 590 nm excitation were carried out by using a different apparatus (see Experimental Section). These experiments, although performed in a spectral window (400−800 nm) limited by the experimental setup (see Experimental Section), have two important advantages: (i) selective excitation of Al-porphyrin chromophore and (ii) analysis of the 530−570 nm spectral region not accessible in the previous experiments (vide supra). The transient absorption spectra following excitation at 590 nm are shown in Figure 8. The initial spectrum (t = 1 ps) is, as expected, the spectrum of the singlet excited **AlMPyP** component.

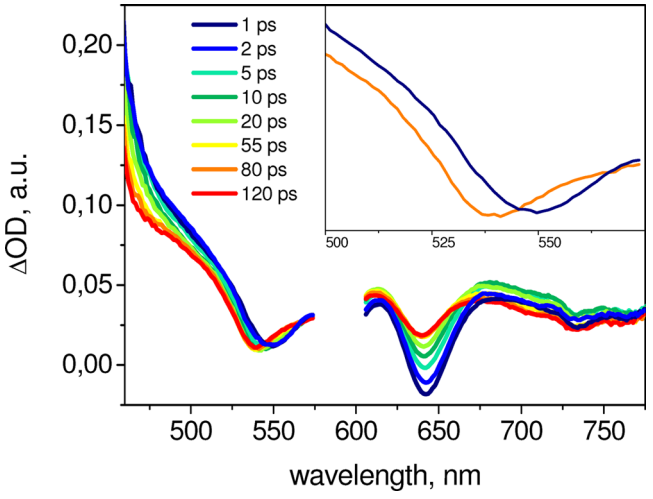

Figure 8. Ultrafast spectroscopy of **C_{60}-AlMPyP-RuP** in dichloromethane (590 nm excitation) in the 1−120 ps time range. Inset: transient absorption spectra at 1 ps (blue line) and 80 ps (orange line) after the excitation.

Particularly informative are the transient spectral changes in the 1−120 ps time range that show a biphasic behavior taking place in the 1−20 ps and in the 20−120 ps range. The early changes (a strong reduction in the bleach of emission at 640 nm accompanied by an increase in the optical density in the 680−700 nm range due to the radical cation of **AlMPyP**) are consistent with an electron transfer mechanism for the quenching of excited **AlMPyP** unit leading to the formation of the Ru-Al^+-C_{60}^- charge separate state. In the subsequent time scale (20−120 ps), the most evident feature is a displacement of the sharp bleach, originally present at 550 nm, toward 530 nm (see inset of Figure 8). As these wavelengths are typical of the Q-bands of the **AlMPyP** and **RuP** units, we can safely assign the bleach displacement to the hole shift from the **AlMPyP** to **RuP** unit [i.e., to the secondary charge separation step (Ru-Al^+-C_{60}^- → Ru^+-Al-C_{60}^-)]. The kinetic analysis of the spectral changes at 680 nm yields time constants of 10 ± 5 ps and 80 ± 5 ps for the first electron transfer and for the hole transfer step, respectively (Figure S9). In the longer time scale (120−2000 ns), the transient changes do not appreciably decay, clearly indicating that the long-range charge-separated state (Ru^+-Al-C_{60}^-) has a lifetime longer than the 2 ns (time window of the instrument). In conclusion, all these results (590 nm excitation) are in reasonable agreement with those obtained by excitation at 550 nm (vide supra), giving strong support to the proposed quenching mechanism.

Since the energy of the charge-separated states depends on the solvent polarity, the photophysical characterization of the triad was repeated in solvents of lower polarity (THF, dielectric constant ε = 7.6, and toluene, ε = 2.4) compared to CH_2Cl_2 (ε = 8.9). Stationary emission measurements clearly indicate that in both solvents, as in CH_2Cl_2, the fluorescence of the Al porphyrin is almost completely quenched. Ultrafast experiments were performed by using 550 nm as excitation wavelength for both solvents. The spectral changes obtained in THF (Figure S10) are qualitatively similar to those observed in CH_2Cl_2, indicating that, following excitation of **AlMPyP** unit, the same sequence of electron transfer processes (oxidative quenching of excited **AlMPyP** unit followed by slower hole transfer step with formation of the long-range charge-separated state) also occurs in this solvent, albeit with somewhat slower kinetics. The values of the time constants obtained from a kinetic analysis at different wavelengths are reported in Table 2. When the solvent was changed to toluene, on the other hand, the results of the ultrafast measurements are somewhat different and can be rationalized by considering the energy level diagram shown in Figure 9 where, since the solvent polarity substantially decreases from CH_2Cl_2 to toluene, the energy of the charge separated states rises.[62] The comparison with the analogous scheme for dichloromethane (Figure 5) clearly suggests that the change in the photophysical mechanism is caused by the change in energy of the charge-separated states.

Table 2. Time Constants (τ) for the Charge Transfer Processes in Different Solvents

	ε^a	τ_1 (ps)^b	τ_2 (ps)^c
CH_2Cl_2	8.9	10	75
THF	7.6	20	80
Toluene	2.4	15	90

[a]Solvent dielectric constant. [b]Time constant of the primary charge separation. [c]Time constant of the hole transfer process.

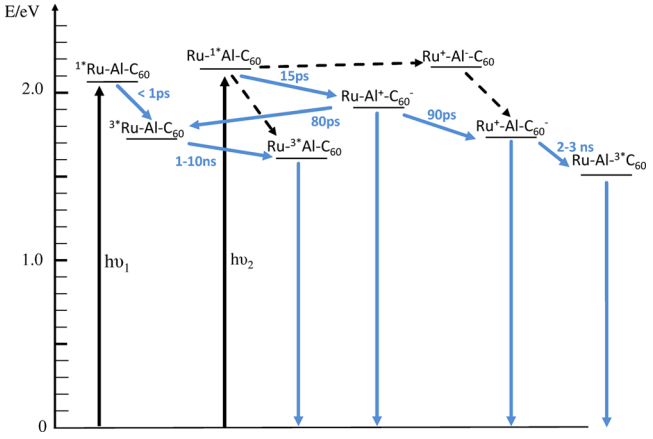

Figure 9. Energy level and photophysical mechanisms for the **C_{60}–AlMPyP–RuP** triad in toluene.

The ultrafast results obtained in toluene are reported in Figure 10. In the first 30 ps (Figure 10a), the transient spectra display spectral features that are qualitatively very similar to those observed in CH_2Cl_2 (decrease in absorption features at 450 and 1240 nm of **AlMPyP** singlet excited state and formation of a wide absorption at 1020 nm due to C_{60}^-), consistent with a fast photoinduced electron transfer step from the singlet excited state of the **AlMPyP** chromophore to the fullerene unit. This step is slightly slower (ca. 15 ps) with respect to CH_2Cl_2 (Figure 11a). In the subsequent time range (30–300 ps, Figure 10b), together with a slight decrease in the C_{60}^- signal at 1000 nm, an increase in the absorption at 850 nm is observed. This signal can be tentatively assigned to the triplet of the Ru-based component formed by charge recombination from the charge transfer state Ru-Al$^+$-C_{60}^-.[63,64] This charge recombination process occurs in ca. 80 ps (Figure 11b) in competition with the hole transfer process Ru-Al$^+$-C_{60}^- → Ru$^+$-Al-C_{60}^-.

In the longer time scale (200–5500 ns, Figure 10c), a new absorption broad band is observed in the 650–750 nm range that directly correlates with the disappearance of the signal at 1020 nm of the C_{60}^-. This band can be assigned to the formation of the fullerene triplet from the charge separated state, Ru$^+$-Al-C_{60}^-, that occurs in competition with the recombination process to the ground state in ca. 2–3 ns (Figure 11c).

The whole set of processes taking place within the triad in toluene are summarized in the energy diagram of Figure 9. In conclusion, kinetic analysis of the spectral changes in toluene gives the values of time constants for the primary charge separation and for the hole transfer reported in Table 2. A comparison between the kinetic behaviors obtained by the photophysical investigation of the triad in different solvents (Table 2), indicates that, while the primary photoinduced charge separation process (τ_1) is very fast (10–20 ps) in all

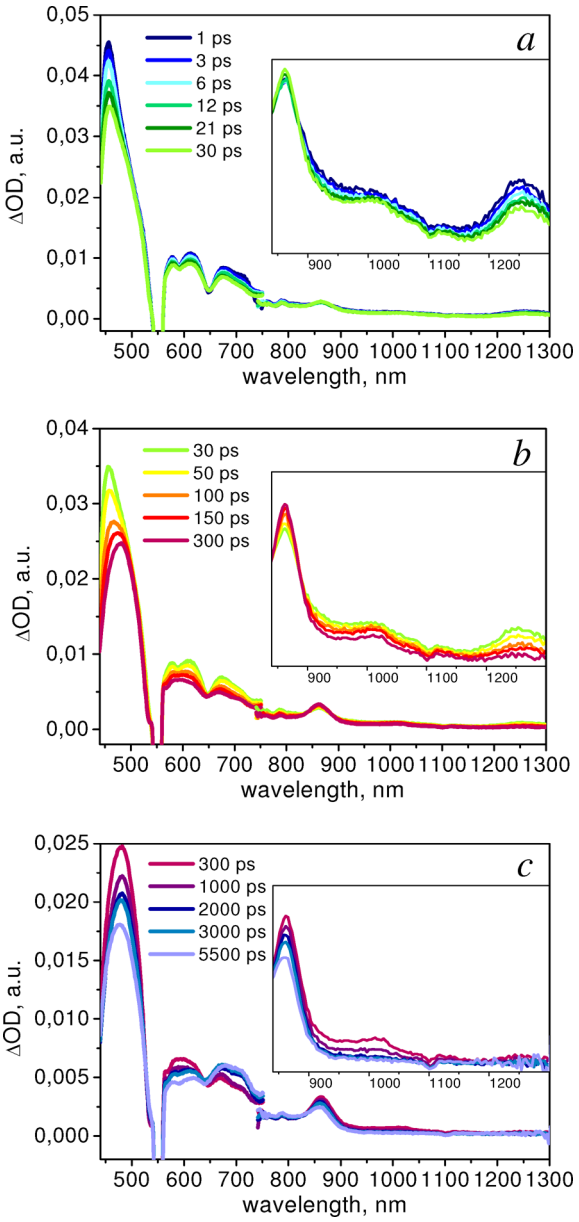

Figure 10. Transient absorption spectra obtained by the ultrafast spectroscopy (excitation at 550 nm) in toluene in the (a) 0–30 ps time range, (b) 30–300 ps range, and (c) 300–5500 ps range. Inset: the transient spectra in the 840–1300 nm spectral window are multiplied by a factor of 10.

solvents investigated, the hole transfer process is slower with time constants slightly increasing with decreasing solvent polarity.

The solvent dependence of the electron transfer kinetics is generally explained in terms of the Marcus theory as a consequence of the combined effects of the driving force and reorganizational energy.[61] However, in our study, it is difficult to make a quantitative comparison since, while in CH_2Cl_2, the energies of the charge-separated states are obtained from redox potentials experimentally measured (Table 1), the energy values in THF and toluene are only estimated and, as a consequence, affected by a large error.

Of particular interest to the present work is the comparison with one of the triad systems studied by van der Est and co-workers,[30] containing aluminium(III) porphyrin as central

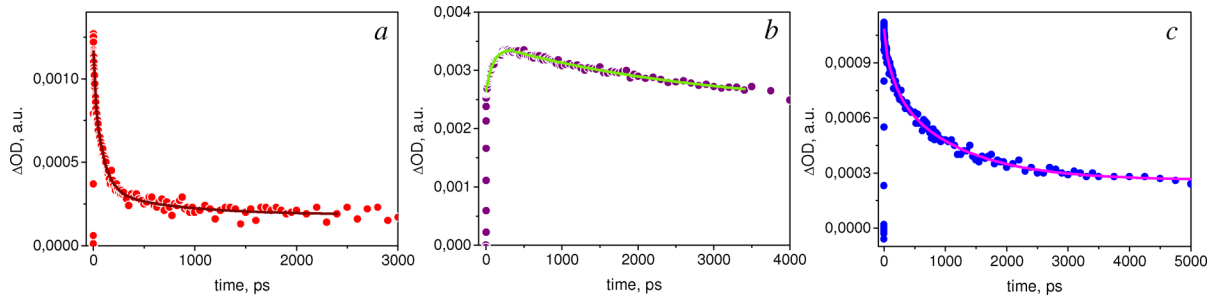

Figure 11. Kinetic analysis of the spectral changes in toluene at (a) 1240 nm, (b) 870 nm, and (c) 1003 nm.

photoexcitable chromophore axially bound to a C_{60} unit and a tetrathiafulvalene (TTF) as an electron-acceptor and electron donor units, respectively (Chart 3). Although the energetics of this system are different because TTF component is a better electron-acceptor than **RuP** component, we can highlight some similarities: (i) a sequential electron transfer (photoinduced electron transfer followed by a charge shift process) is observed with a far faster charge separation than the charge recombination process, and (ii) in toluene, the triplet state of the C_{60} unit is involved in the deactivation of the excited **AlMPyP** chromophoric component. We can, however, observe that van der Est's triad exhibits a better performance featuring a slightly longer lifetime of the charge-separated state (64 ns) than that measured for our system (ca.10−20 ns). One of the factors that most likely determines this behavior is a longer distance between the donor and acceptor units, together with the linear spatial arrangement which ensures that the donor and acceptor units are spatially well-separated.

Chart 3. Triad System Studied by van der Est[30]

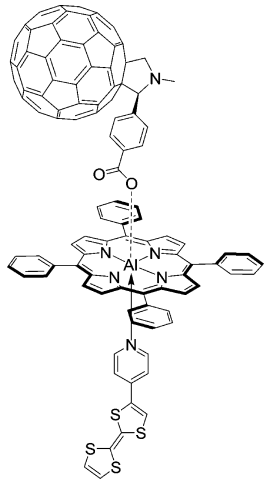

CONCLUSION

In this work, the supramolecular triad, **C_{60}-AlMPyP-RuP**, is successfully synthesized by a self-assembling synthetic method. The photophysical behavior, following light absorption by **AlMPyP** chromophore, has been thoroughly investigated by time-resolved emission and absorption techniques in the femtosecond−nanosecond time domain in different solvents, with particular regard to the photoinduced charge separation and recombination processes. The results provide evidence for the occurrence of stepwise electron/hole transfer, leading to a charge-separated state with reduced fullerene acceptor and oxidized ruthenium porphyrin donor, with a lifetime in the few nanoseconds range. Although the charge-separating performance of this triad is not outstanding, particularly because of the relatively short charge separation distance, this study demonstrates that, by using a self-assembling strategy, improvements can be made by appropriate chemical modifications of the individual molecular components.

AUTHOR INFORMATION

Corresponding Authors

*E-mail: idm@unife.it.

*E-mail: eiengo@units.it.

ORCID

Maria Teresa Indelli: 0000-0002-8048-4441

Author Contributions

The manuscript was written through contributions of all authors. All authors have given approval to the final version of the manuscript.

Notes

The authors declare no competing financial interest.

ACKNOWLEDGMENTS

The authors acknowledge Dr. Claudio Chiorboli (University of Ferrara, Italy) for the time-resolved ultrafast measurements (590 nm excitation) in the visible region and Prof. T. Da Ros (University of Trieste, Italy) for the initial help in the preparation of the fullerene derivative. Financial support from the Italian MIUR (FIRB RBAP11C58Y "NanoSolar", PRIN 2010 "Hi-Phuture") and from the University of Trieste (FRA2016, Fondo di Ricerca di Ateneo) are gratefully acknowledged. A.K. gratefully acknowledges funding from the Deutsche Forschungsgemeinschaft (DFG) via Grant KA 3491/2-1.

REFERENCES

(1) Lewis, N. S.; Nocera, D. G. Powering the Planet: Chemical Challenges in Solar Energy Utilization. *Proc. Natl. Acad. Sci. U. S. A.* **2006**, *103*, 15729−15735.

(2) Barber, J. Photosynthetic Energy Conversion: Natural and Artificial. *Chem. Soc. Rev.* **2009**, *38*, 185−196.
(3) Cook, T. R.; Dogutan, D. K.; Reece, S. Y.; Surendranath, Y.; Teets, T. S.; Nocera, D. G. Solar Energy Supply and Storage for the Legacy and Nonlegacy Worlds. *Chem. Rev.* **2010**, *110*, 6474−6502.
(4) Gust, D.; Moore, T. A.; Moore, A. L. Realizing Artificial Photosynthesis. *Faraday Discuss.* **2012**, *155*, 9−26.
(5) Frischmann, P. D.; Mahata, K.; Würthner, F. Powering the Future of Molecular Artificial Photosynthesis with Light-harvesting Metallosupramolecular Dye Assemblies. *Chem. Soc. Rev.* **2013**, *42*, 1847−1870.
(6) Kärkäs, M. D.; Johnston, E. V.; Verho, O.; Åkermark, B. Artificial Photosynthesis: from Nanosecond Electron Transfer to Catalytic Water Oxidation. *Acc. Chem. Res.* **2014**, *47*, 100−111.
(7) Gust, D. Supramolecular Photochemistry Applied to Artificial Photosynthesis and Molecular Logic Devices. *Faraday Discuss.* **2015**, *185*, 9−35.
(8) Natali, M.; Scandola, F. In *Supramolecular Artificial Photosynthesis*; Bergamini, G., Silvi, S., Ed.; Applied Photochemistry, Lecture Notes in Chemistry; Springer, 2016, Vol. *92*, DOI: 10.1007/978-3-319-31671-0_1.
(9) Kim, D. *Multiporphyrin Arrays: Fundamentals and Applications*; Pan Stanford Publishing, CRC Press, 2012.
(10) Yong, C. K.; Parkinson, P.; Kondratuk, D. V.; Chen, W. H.; Stannard, A.; Summerfield, A.; Sprafke, J. K.; O'Sullivan, M. C.; Beton, P. H.; Anderson, H. L.; et al. Ultrafast Delocalization of Excitation in Synthetic Light-harvesting Nanorings. *Chem. Sci.* **2015**, *6*, 181−189.
(11) Kodis, G.; Terazono, Y.; Liddell, P. A.; Andrèasson, J.; Garg, V.; Hambourger, M.; Moore, T. A.; Moore, A. L.; Gust, D. Energy and Photoinduced Electron Transfer in a Wheel-Shaped Artificial Photosynthetic Antenna-Reaction Center Complex. *J. Am. Chem. Soc.* **2006**, *128*, 1818−1827.
(12) Aratani, N.; Kim, D.; Osuka, A. Discrete Cyclic Porphyrin Arrays as Artificial Light-Harvesting Antenna. *Acc. Chem. Res.* **2009**, *42*, 1922−1934.
(13) Kuramochi, Y.; Sandanayaka, A. S. D.; Satake, A.; Araki, Y.; Ogawa, K.; Ito, O.; Kobuke, Y. Energy Transfer Followed by Electron Transfer in a Porphyrin Macrocycle and Central Acceptor Ligand: A Model for a Photosynthetic Composite of the Light-Harvesting Complex and Reaction Center. *Chem. - Eur. J.* **2009**, *15*, 2317−2327.
(14) Guldi, D. M. Fullerene−Porphyrin Architectures; Photosynthetic Antenna and Reaction Center Models. *Chem. Soc. Rev.* **2002**, *31*, 22−36.
(15) Serroni, S.; Campagna, S.; Puntoriero, F.; Di Pietro, C.; McClenaghan, N. D.; Loiseau, F. Dendrimers Based on Ruthenium(II) and Osmium(II) Polypyridine Complexes and the Approach of Using Complexes as Ligands and Complexes as Metals. *Chem. Soc. Rev.* **2001**, *30*, 367−375.
(16) Fukuzumi, S.; Ohkubo, K.; Suenobu, T. Long-Lived Charge Separation and Applications in Artificial Photosynthesis. *Acc. Chem. Res.* **2014**, *47*, 1455−1464.
(17) Imahori, H.; Guldi, D. M.; Tamaki, K.; Yoshida, Y.; Luo, C.; Sakata, Y.; Fukuzumi, S. Charge Separation in a Novel Artificial Photosynthetic Reaction Center Lives 380 ms. *J. Am. Chem. Soc.* **2001**, *123*, 6617−6628.
(18) Ngo, T. H.; Zieba, D.; Webre, W. A.; Lim, G. N.; Karr, P. A.; Kord, S.; Jin, S.; Ariga, K.; Galli, M.; Goldup, S.; et al. Engaging Copper(III) Corrole as an Electron Acceptor: Photoinduced Charge Separation in Zinc Porphyrin−Copper Corrole Donor−Acceptor Conjugates. *Chem. - Eur. J.* **2016**, *22*, 1301−1312.
(19) Wasielewski, M. R. Self-Assembly Strategies for Integrating Light Harvesting and Charge Separation in Artificial Photosynthetic Systems. *Acc. Chem. Res.* **2009**, *42*, 1910−1921.
(20) Guldi, D. M.; Imahori, H.; Tamaki, K.; Kashiwagi, Y.; Yamada, H.; Sakata, Y.; Fukuzumi, S. A Molecular Tetrad Allowing Efficient Energy Storage for 1.6 s at 163 K. *J. Phys. Chem. A* **2004**, *108*, 541−548.
(21) Iengo, E.; Zangrando, E.; Alessio, E. Synthetic Strategies and Structural Aspects of Metal-Mediated Multiporphyrin Assemblies. *Acc. Chem. Res.* **2006**, *39*, 841−851.
(22) Scandola, F.; Chiorboli, C.; Prodi, A.; Iengo, E.; Alessio, E. Photophysical properties of metal-mediated assemblies of porphyrins. *Coord. Chem. Rev.* **2006**, *250*, 1471−1496.
(23) Iengo, E.; Pantos, G. D.; Sanders, J. K. M.; Orlandi, M.; Chiorboli, C.; Fracasso, S.; Scandola, F. A Fully Self-Assembled Nonsymmetric Triad for Photoinduced Charge Separation. *Chem. Sci.* **2011**, *2*, 676−685.
(24) Gatti, T.; Cavigli, P.; Zangrando, E.; Iengo, E.; Chiorboli, C.; Indelli, M. T. Improving the Efficiency of the Photoinduced Charge-Separation Process in a Rhenium(I)−Zinc Porphyrin Dyad by Simple Chemical Functionalization. *Inorg. Chem.* **2013**, *52*, 3190−3197.
(25) Iengo, E.; Cavigli, P.; Gamberoni, M.; Indelli, M. T. A Selective Metal-Mediated Approach for the Efficient Self-Assembling of Multi-Component Photoactive Systems. *Eur. J. Inorg. Chem.* **2014**, *2014*, 337−344.
(26) Cavigli, P.; Da Ros, T.; Kahnt, A.; Gamberoni, M.; Indelli, M. T.; Iengo, E. Zinc Porphyrin−Re(I) Bipyridyl−Fullerene Triad: Synthesis, Characterization, and Kinetics of the Stepwise Electron-Transfer Processes Initiated by Visible Excitation. *Inorg. Chem.* **2015**, *54*, 280−292.
(27) Poddutoori, P. K.; Sandanayaka, A. S. D.; Hasobe, T.; Ito, O.; van der Est, A. Photoinduced Charge Separation in a Ferrocene−Aluminum(III) Porphyrin−Fullerene Supramolecular Triad. *J. Phys. Chem. B* **2010**, *114*, 14348−14357.
(28) Poddutoori, P. K.; Sandanayaka, A. S. D.; Zarrabi, N.; Hasobe, T.; Ito, O.; van der Est, A. Sequential Charge Separation in Two Axially Linked Phenothiazine−Aluminum(III) Porphyrin−Fullerene Triads. *J. Phys. Chem. A* **2011**, *115*, 709−717.
(29) Poddutoori, P. K.; Bregles, L. P.; Lim, G. N.; Boland, P.; Kerr, R. G.; D'Souza, F. Modulation of Energy Transfer into Sequential Electron Transfer upon Axial Coordination of Tetrathiafulvalene in an Aluminum(III) Porphyrin−Free-Base Porphyrin Dyad. *Inorg. Chem.* **2015**, *54*, 8482−8494.
(30) Poddutoori, P. K.; Lim, G. N.; Sandanayaka, A. S. D.; Karr, P. A.; Ito, O.; D'Souza, F.; Pilkington, M.; van der Est, A. Axially Assembled Photosynthetic Reaction Center Mimics Composed of Tetrathiafulvalene, Aluminum(III) Porphyrin and Fullerene Entities. *Nanoscale* **2015**, *7*, 12151−12165.
(31) Da Ros, T.; Prato, M.; Guldi, D. M.; Ruzzi, M.; Pasimeni, L. Efficient Charge Separation in Porphyrin-Fullerene-Ligand Complexes. *Chem. - Eur. J.* **2001**, *7*, 816−827.
(32) Schuster, D. I.; Li, K.; Guldi, D. M.; Palkar, A.; Echegoyen, L.; Stanisky, C.; Cross, R. J.; Niemi, M.; Tkachenko, N. V.; Lemmetyinen, H. Azobenzene-Linked Porphyrin−Fullerene Dyads. *J. Am. Chem. Soc.* **2007**, *129*, 15973−15982.
(33) Garg, V.; Kodis, G.; Chachisvilis, M.; Hambourger, M.; Moore, A. L.; Moore, T. A.; Gust, D. Conformationally Constrained Macrocyclic Diporphyrin−Fullerene Artificial Photosynthetic Reaction Center. *J. Am. Chem. Soc.* **2011**, *133*, 2944−2954.
(34) Bottari, G.; Trukhina, O.; Ince, M.; Torres, T. Towards Artificial Photosynthesis: Supramolecular, Donor−Acceptor, Porphyrin- and Phthalocyanine/Carbon Nanostructure Ensembles. *Coord. Chem. Rev.* **2012**, *256*, 2453−2477.
(35) Wijesinghe, C. A.; El-Khouly, M. E.; Zandler, M. E.; Fukuzumi, S.; D'Souza, F. A Charge-Stabilizing, Multimodular, Ferrocene−Bis(triphenylamine)−Zinc-porphyrin−Fullerene Polyad. *Chem. - Eur. J.* **2013**, *19*, 9629−9638.
(36) Possamai, G.; Menna, E.; Maggini, M.; Carano, M.; Marcaccio, M.; Paolucci, F.; Guldi, D. M.; Swartz, A. Rhenium(I) and Ruthenium(II) Complexes with a Crown-linked Methanofullereneligand: Synthesis, Electrochemistry and Photophysical Characterization. *Photochem. Photobiol. Sci.* **2006**, *5*, 1154−1164.
(37) Karlsson, S.; Modin, J.; Becker, H.-C.; Hammarström, L.; Grennberg, H. How Close Can You Get? Studies of Ultrafast Light-Induced Processes in Ruthenium-[60] Fullerene Dyads with Short Pyrazolino and Pyrrolidino Links. *Inorg. Chem.* **2008**, *47*, 7286−7294.

(38) Iehl, J.; Vartanian, M.; Holler, M.; Nierengarten, J.-F.; Delavaux-Nicot, B.; Strub, J.-M.; Van Dorsselaer, A.; Wu, Y.; Mohanraj, J.; Yoosaf, K.; et al. Photoinduced Electron Transfer in a Clicked Fullerene–Porphyrin Conjugate. *J. Mater. Chem.* **2011**, *21*, 1562–1573.
(39) Walsh, E. A.; Deye, J. R.; Baas, W.; Sullivan, K.; Lancaster, A.; Walters, K. A. Synthesis and Spectroscopic Studies of Transition-Metal Fullerene Supramolecular Systems. *J. Photochem. Photobiol., A* **2013**, *260*, 24–36.
(40) Obondi, C. O.; Lim, G. N.; D'Souza, F. Triplet–Triplet Excitation Transfer in Palladium Porphyrin–Fullerene and Platinum Porphyrin–Fullerene Dyads. *J. Phys. Chem. C* **2015**, *119*, 176–185.
(41) Chandra, B. KC; Lim, G. N.; D'Souza, F. Multi-modular, Tris(triphenylamine) Zinc Porphyrin–Zinc Phthalocyanine–Fullerene Conjugate as a Broadband Capturing, Charge Stabilizing, Photosynthetic 'Antenna-Reaction Center' Mimic. *Nanoscale* **2015**, *7*, 6813–6826.
(42) Martín, N.; Sánchez, L.; Illescas, B.; Pérez, I. C_{60}-Based Electroactive Organofullerenes. *Chem. Rev.* **1998**, *98*, 2527–2548.
(43) Guldi, D. M.; Prato, M. Excited-State Properties of C_{60} Fullerene Derivatives. *Acc. Chem. Res.* **2000**, *33*, 695–703.
(44) Nastasi, F.; Puntoriero, F.; Natali, M.; Mba, M.; Maggini, M.; Mussini, P.; Panigati, M.; Campagna, S. Photoinduced Intercomponent Excited-State Decays in a Molecular Dyad Made of a Dinuclear Rhenium(I) Chromophore and a Fullerene Electron Acceptor Unit. *Photochem. Photobiol. Sci.* **2015**, *14*, 909–918.
(45) Obondi, C. O.; Lim, G. N.; Churchill, B.; Poddutoori, P. K.; van der Est, A.; D'Souza, F. Modulating the Generation of Long-lived Charge Separated States Exclusively from The Triplet Excited States in Palladium Porphyrin–Fullerene Conjugates. *Nanoscale* **2016**, *8*, 8333–8344.
(46) Fleischer, E. B.; Shachter, A. M. Coordination Oligomers and a Coordination Polymer of Zinc Tetraarylporphyrins. *Inorg. Chem.* **1991**, *30*, 3763–3769.
(47) Alessio, E.; Macchi, M.; Heath, S.; Marzilli, L. G. A Novel Open-box Shaped Pentamer of Vertically Linked Porphyrins that Selectively Recognizes S-bonded Me_2SO Complexes. *Chem. Commun.* **1996**, 1411–1412.
(48) Prodi, A.; Indelli, M. T.; Kleverlaan, C. J.; Scandola, F.; Alessio, E.; Gianferrara, T.; Marzilli, L. Side-to-Face Ruthenium Porphyrin Arrays: Photophysical Behavior of Dimeric and Pentameric Systems. *Chem. - Eur. J.* **1999**, *5*, 2668–2679.
(49) Davidson, G. J. E.; Tong, L. H.; Raithby, P. R.; Sanders, J. K. M. Aluminium(III) Porphyrins as Supramolecular Building Blocks. *Chem. Commun.* **2006**, 3087–3089.
(50) Chiorboli, C.; Rodgers, M. A. J.; Scandola, F. Ultrafast Processes in Bimetallic Dyads with Extended Aromatic Bridges. Energy and Electron Transfer Pathways in Tetrapyridophenazine-Bridged Complexes. *J. Am. Chem. Soc.* **2003**, *125*, 483–491.
(51) The absorption spectrum shows a weak tail at long wavelength observed in related complexes and tentatively assigned to a weak charge transfer interaction between the porphyrin and fullerene.[28]
(52) From this fact, we can rule out energy transfer as an effective quenching mechanism of AlP fluorescence.
(53) A relatively long-lived component (lifetime, 1–5 ns) arising from impurities of unquenched aluminium porphyrin species is observed.
(54) The energies of the localized excited states of the Ru-based,[23] Al-based,[28] and fullerene units[55] have been taken from the literature and are independent of the solvent.
(55) Luo, C.; Guldi, D. M.; Imahori, H.; Tamaki, K.; Sakata, K. Sequential Energy and Electron Transfer in an Artificial Reaction Center: Formation of a Long-Lived Charge-Separated State. *J. Am. Chem. Soc.* **2000**, *122*, 6535–6551.
(56) In this CH_2Cl_2 diagram, the excited states localized on the C_{60} unit have been omitted because the contribution of this unit to the visible absorption is totally negligible and, moreover, in CH_2Cl_2, the singlet and triplet states of this unit are practically not involved in the photophysical deactivation of the triad.
(57) Rehm, D.; Weller, A. Kinetic and Mechanism of Electron Transfer in Fluorescence Quenching in Acetonitrile. *Ber. Bunsen-Ges. Phys. Chem.* **1969**, *73*, 834–839.
(58) In the calculation of the work term, an average value of 10 Å has been assumed for centre-to-centre distances between the molecular units.
(59) Since the excitation at 550 nm is not selective (a fraction of light, ca. 30%, is absorbed by RuP component), in the initial spectrum (t = 1 ps) an absorption is present at around 850 nm, characteristic of the triplet of the RuP component formed by prompt intersystem crossing following direct excitation.[48] This signal decays in a long time scale (>5000 ps) according to that observed in a previous paper.[25]
(60) Nanosecond laser flash photolysis experiments could be useful to measure the rate constant of charge recombination process, but with the our apparatus, the excitation at 550 nm is not feasible.
(61) Marcus, R. A.; Sutin, N. Electron Transfer in Chemistry and Biology. *Biochim. Biophys. Acta, Rev. Bioenerg.* **1985**, *811*, 265–322.
(62) A rough estimation of the energy of the charge-separated states in toluene can be obtained by the correction of the experimental redox potentials measured in CH_2Cl_2 using an appropriate work term.[57]
(63) The charge transfer state ($RuP\text{-}AlP^{+}\text{-}C_{60}^{-}$), initially formed in a singlet spin state, can undergo spin inversion and yields Ru-based triplet state upon charge recombination.[64] The Ru-based triplet state, as reported in the literature,[25] is expected to undergo a fast triplet–triplet energy transfer to AlP-based unit.
(64) Ghirotti, M.; Chiorboli, C.; You, C. C.; Wurthner, F.; Scandola, F. Photoinduced Energy and Electron-Transfer Processes in Porphyrin–Perylene Bisimide Symmetric Triads. *J. Phys. Chem. A* **2008**, *112*, 3376–3385.